University of Groningen

Exploring the Biocatalytic Potential of a Self-Sufficient Cytochr ome P450 from Thermothelomyces thermophila

Fürst, Maximilian; Kerschbaumer, Bianca; Rinnofner, Claudia; Migglautsch, Anna; Winkler, Margit; Fraaije, Marco

IMPORTANT NOTE: You are advised to consult the publisher's version (publisher's PDF) if you wish to cite from it. Please check the document version below.

Document Version
Version created as part of publication process; publisher's layout; not normally made publicly available

[Link to publication in University of Groningen/UMCG research database](#)

Exploring the Biocatalytic Potential of a Self-Sufficient Cytochrome P450 from *Thermothelomyces thermophila*

Maximilian J. L. J. Fürst,[a] Bianca Kerschbaumer,[b] Claudia Rinnofner,[b, c] Anna K. Migglautsch,[d] Margit Winkler,[b] and Marco W. Fraaije[a,]*

[a] Molecular Enzymology Group, University of Groningen, Nijenborgh 4, 9747AG, Groningen, The Netherlands
     Tel: (+31)-50-36-34345
     E-mail: m.w.fraaije@rug.nl
[b] Austrian Centre of Industrial Biotechnology (ACIB), Petersgasse 14, 8010 Graz, Austria
[c] Bisy e.U., Wetzawinkel 20, 8200 Hofstätten/Raab, Austria
[d] Institute of Organic Chemistry, Graz University of Technology, NAWI Graz, 8010 Graz, Austria

Supporting information for this article is available on the WWW under https://doi.org/10.1002/adsc.201900076

Abstract: Among nature's arsenal of oxidative enzymes, cytochrome P450s (CYPs) catalyze the most challenging reactions, the hydroxylations of non-activated C–H bonds. Human CYPs are studied in drug development due to their physiological role at the forefront of metabolic detoxification, but their challenging handling makes them unsuitable for application. CYPs have a great potential for biocatalysis, but often lack appropriate features such as high and soluble expression, self-sufficient internal electron transport, high stability, and an engineerable substrate scope. We have probed these characteristics for a recently described CYP that originates from the thermophilic fungus *Thermothelomyces thermophila* (CYP505A30), a homolog of the well-known P450-BM3 from *Bacillus megaterium*. CYP505A30 is a natural monooxygenase-reductase fusion, is well expressed, and moderately tolerant towards temperature and solvent exposure. Although overall comparable, we found the stability of the enzyme's domains to be inverse to P450-BM3, with a more stable reductase compared to the heme domain. After analysis of a homology model, we created mutants of the enzyme based on literature data for P450-BM3. We then probed the enzyme variants in bioconversions using a panel of active pharmaceutical ingredients, and activities were detected for a number of structurally diverse compounds. Ibuprofen was biooxidized in a preparative scale whole cell bioconversion to 1-, 2- and 3-hydroxyibuprofen.

Keywords: active pharmaceutical ingredient; biocatalysis; heme proteins; hydroxylation; ibuprofen; oxygenation; self-sufficient cytochrome P450

Introduction

One of the most challenging reactions in organic chemistry is the oxidation of non-activated carbons. Overcoming the inertness of C–C and C–H bonds requires very high reaction temperatures or highly reactive chemical species, commonly resulting in energy intensive and poorly controllable processes.[1] In nature, ubiquitously found enzymes called cytochrome P450s (CYPs or P450s) use molecular oxygen as the oxidant to perform various oxidation reactions (hydroxylations, dealkylations, heteroatom oxidations and epoxidations), while forming water as the byproduct.[2] Initially, CYPs were studied in humans: acting as a phase I metabolic frontier, P450s oxidize xenobiotics to increase their solubility and activate them for further metabolism.[3] With the majority of drugs being direct substrates, the comprehension of CYPs is of paramount importance in clinical and pharmaceutical science. However, the physiologically
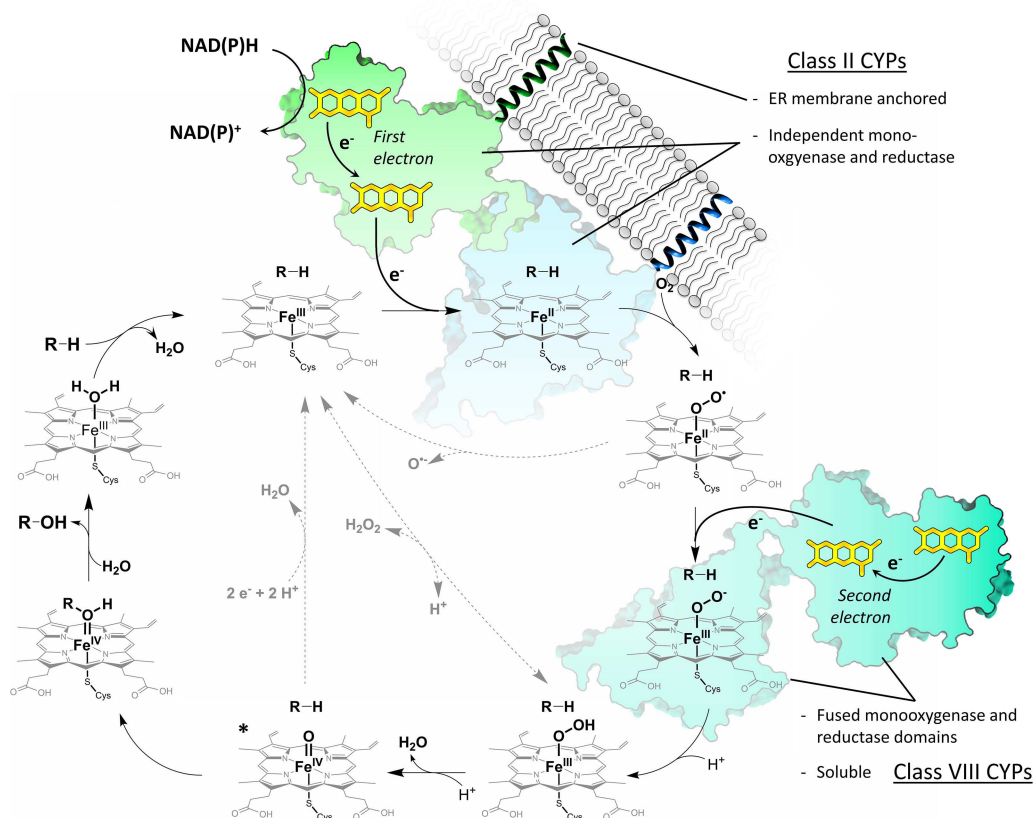
Scheme 1. Catalytic cycle of cytochrome P450s[5] (CYPs) and comparison of membrane-bound Class II (depicted in the first electron transfer step) and soluble class VIII CYPs (depicted for the second electron transfer step).[6] In both classes, the two required electrons originate from a hydride transferred from NAD(P)H. The electron acceptor is a flavin cofactor in a cytochrome P450 reductase, which is either a separate enzyme (class II) or a fused domain (class VIII). The electrons are successively shuttled to the heme via a second flavin, allowing first the reaction with dioxygen and then the maturation to the catalytically active "compound I" (marked by *). Uncoupling pathways (grey dashed lines) can lead to the formation of reactive oxygen species.

obligatory substrate promiscuity rendered them also as valuable biocatalysts for the selective oxidation of non-activated carbons under mild process conditions.[4]

The complex reaction mechanism (Scheme 1) enabling the remarkable chemistry of P450s involves a heme prosthetic group, whose porphyrin ring coordinates an iron atom that is proximally ligated to a cysteine. If a suitable substrate enters the active site, it displaces an axial water molecule and triggers the reductive activation of oxygen. Electrons from a nicotinamide cofactor (NADPH or NADH) are successively shuttled through a reductase system to the heme. The one electron-reduced ferrous state binds dioxygen and the second electron creates the ferric peroxy complex. Protonation and water elimination yields "Compound I", which reacts with the substrate through a radical-rebound mechanism.[2]

Unproductive pathways shortcutting this principle cycle lead to the uncoupling of electron consumption from product formation and can create hydrogen peroxide (H_2O_2) or superoxide. This characteristic can be exploited to drive the reaction reverse using excess

H_2O_2, leading to a cofactor-avoiding shunt pathway.[7] In nature, most often an FAD-containing reductase acts as the hydride acceptor, and a ferredoxin or flavodoxin as the single electron mediator. The individual components can exist as separate, or as fused, multidomain proteins ("self-sufficient"). The various possible combinations differentiate the CYP subclasses. In bacteria, the CYP system is typically cytosolic, while it is membrane-bound in eukaryotes.[6] For this reason, the physiologically relevant human CYPs, which are membrane-bound two component systems, are typically isolated in microsomes and their handling is generally challenging.[8] An easier to study model system was found in CYP102A1 (also known as P450-BM3) from *Bacillus megaterium*. P450-BM3 is soluble, all components are fused to one polypeptide, and the single electron mediator is an FMN-containing, flavodoxin-like domain, equivalent to the human microsomal system.[9] Significant advances in understanding CYP's redox transfer mechanisms were made with P450-BM3,[5b] but due to its unprecedented catalytic rate, it was quickly conceived as an out-

standing biocatalyst as well.[10] After the crystal structure was solved,[11] this notion has since been corroborated by the accomplishments in engineering the enzyme to work on countless unnatural substrates. Desired activities are generally either of interest for organic synthesis, e.g. in late stage functionalization,[12] or mimic human drug metabolism. The latter can substantially simplify pharmacokinetic studies, where an access to drug metabolites is required for adverse drug reaction assessments or prodrug studies.[13]

Since many target compounds for P450s are hydrophobic, organic solvent systems commonly need to be applied. In this regard, (industrial) application of CYPs encountered a major hurdle, because they typically suffer from poor stability in these conditions.[14] Besides the use of solvents, industrial processes often run optimally at elevated temperatures to increase reaction rates and compound solubility. Thermo- and solvent stability of proteins often go hand in hand and can be improved simultaneously.[15] Although the mesophilic P450-BM3 is already considerably more stable than e.g. human CYPs,[16] it was engineered toward even higher solvent- and thermostability using random mutagenesis.[17] However, considerable improvements need to be achieved for application of a P450 biocatalyst in most industrial processes.[18]

Here we report on our investigations on a recently characterized CYP from the fungus *Thermothelomyces thermophila* (CYP505A30).[19] This enzyme is of the same class as P450-BM3 and could emerge as an alternative biocatalyst due to its mesophilic nature and distinct substrate scope. We show that CYP505A30's stability is similar to P450-BM3's, but with inverted stability differences between the P450 and reductase domains. Further characterization of the enzyme was conducted and several substrates for the wild-type and mutated variants were identified.

Results and Discussion

Stimulated by our previous experience in identifying biocatalytically interesting oxidoreductases in the thermophilic fungus *Thermothelomyces thermophila*[20] (formerly known as *Myceliophthora thermophila*[21]) we decided to focus on a gene encoding a cytochrome P450-homolog (locus tag MYCTH_101224). Sequence alignment revealed the gene to consist of a single open reading frame for a self-sufficient P450 of 1080 amino acids, identical to CYP505A30.[19] A synthetic and codon-optimized gene was cloned in a pET28a vector conferring an N-terminal 6x histidine tag, and the protein was expressed in *Escherichia coli* BL21 (DE3). Nickel-Sepharose affinity chromatography yielded a protein of approximately 125 kDa, as estimated by SDS-PAGE (Figure S1). The red-brown protein showed a major absorption peak at 415 nm. Upon reduction and

carbon monoxide binding, the characteristic 450 nm soret band was observed. Dodecanoic (lauric) acid was used as a standard substrate. Fast consumption of either NADH or NADPH was observed when followed spectrophotometrically at 340 nm in the presence of 1 μM of enzyme and 1 mM substrate, confirming a catalytically competent and self-sufficient monooxygenase with preference for NADPH, in agreement with what was reported recently.[19] In the absence of an organic substrate, we measured an NADPH oxidation "leak rate" of only 0.02 s^{-1}, significantly lower than the reported values for P450-BM3, which range from 0.083 s^{-1} to 0.5 s^{-1}.[22] GC-MS analysis of the ethyl acetate-extracted and TMS-derivatized reaction mix containing a phosphite dehydrogenase-based NADPH regeneration system[23] confirmed a hydroxylating activity on lauric acid. We found full conversion after 24 h and 86% ω-1 oxidation (Figure S2). A similar result was reported by Baker et al.[19]

We next assessed the thermostability of CYP505A30 under varying conditions by determining its apparent melting temperature (T_m). Using a thermal-shift assay, the unfolding of the entire protein can be monitored by supplementing a dye that exhibits fluorescence upon binding to the exposed hydrophobic core. The T_m is defined as the temperature at the inflection point of the corresponding melting curve.

For CYP505A30, we observed two distinct melting temperatures that differed by approximately 8 °C, attributable to a three-state unfolding. Using principally the same assay, Baker et al. did not observe such an apparent intermediate state, which may be due to the different protocol in temperature ramping. The two T_ms are in good agreement, however, for what they reported as the unfolding temperature of the full protein (58 °C) and a truncated protein consisting of only the heme domain (48 °C), respectively. To establish whether the second maximum corresponds to the reductase domain, we performed the same assay without addition of dye, following the fluorescence of the flavin cofactors instead. As expected, this so-called ThermoFAD method[24] resulted in only one peak for the T_m, which we assigned to the flavin-containing reductase domain (Figure S3). In contrast to P450-BM3, CYP505A30 showed a higher stability for the reductase domain as compared to the heme domain. Figure 1A shows the pH-dependent melting temperatures of the two domains of CYP505A30 in a pH range from 3.6–9. The protein displayed a maximal stability at slightly acidic pH, with the maximum T_m of the reductase domain found to be 56.3 °C at pH 6, and the highest T_m of the heme domain of 49.8 °C at pH 5.6. Although Baker et al. reported a stability maximum at pH 7, Figure 1A shows that CYP505A30 displays a very broad pH stability and a barely changed T_m of the reductase domain in the pH range 5–7.5. This stability is an attractive feature from an application
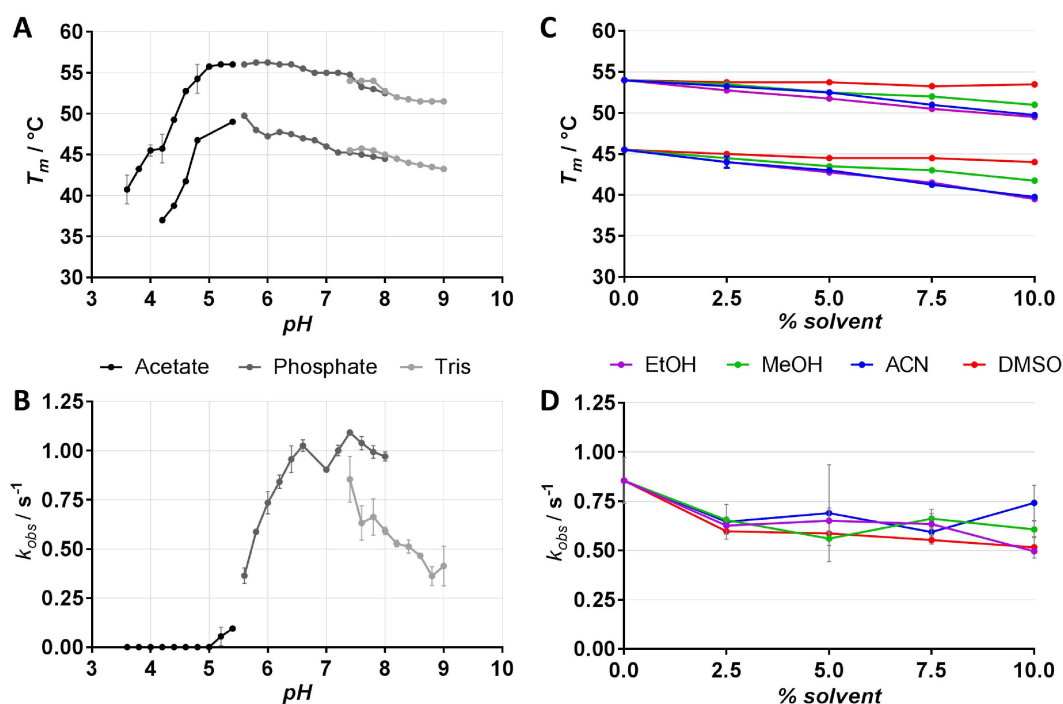
Figure 1. pH profile and solvent tolerance of CYP505A30. As the enzyme exhibits two distinct unfolding events, two T_m data sets are plotted in (A) and (C). The higher stability curve can be assumed to correspond to the reductase domain, as it matches the profile found when following the fluorescent flavin cofactor of this domain (Figure S3). pH profiles (A and B) were determined in 50 mM Na$^+$ acetate, Na$^+$ phosphate or Tris/HCl buffers, indicated in shades of grey. Solvent tolerance (C and D) was measured in Tris/HCl at pH 7.4 in the presence of varying amounts of ethanol, methanol, acetonitrile and DMSO, indicated by various colors. Activity measurements (B and D) were conducted in presence of 100 μM NADPH and 1 mM lauric acid.

point of view and one that also facilitates kinetic studies and the investigation of protonation states in the electron transfer reactions. When comparing the T_ms to literature data, we found them to be similar to P450-BM3, which showed three distinct peaks of 48°C, 58.4°C and 63°C in a differential scanning calorimetry assay.[16] In the case of P450-BM3, however, the reductase domain corresponds to the lowest unfolding temperature. With the distinct (potentially irreversible) unfolding event at 58.4°C likely being deleterious to the heme domain's activity, CYP505A30 and P450-BM3 basically inactivate at the same temperatures, although with an inversion of the unfolding order of the domains. Because stability is not necessarily correlated to catalytic activity, we also determined a pH profile of apparent activity by measuring NADPH consumption in the same pH range as before (Figure 1B). The pH range of oxidation activity was found to be more narrow and similar to what was described for P450-BM3.[25] In contrast to the stability optimum, the enzyme was found to oxidize the cofactor fastest at pH 7.4, about 1.5 pH units above the stability optimum.

To further assess the stability and applicability of CYP505A30, we also measured the T_m and NADPH consumption in the presence of various cosolvents.

With increasing solvent levels, we found an approximately linear decrease of stability. The effect was relatively limited and depended on the type of solvent. The strongest effect was measured with 10% ethanol, which decreased the T_m of both domains by 6°C, while DMSO had the least influence and decreased the T_m by only 1.5°C at 10%. Moreover, the apparent activity decreased only marginally in the presence of cosolvents, and at comparable rates for all solvents used.

In order to investigate CYP505A30's suitability as a biocatalyst, we next looked at the enzyme's ability to perform reactions of value. One reason why P450-BM3 gained high interest in the field of biocatalysis was the successes in engineering the enzyme to accept pharmaceutical compounds. In the absence of a crystal structure, we first created a homology model of the catalytic heme domain, using YASARA (Figure 2). P450-BM3 was automatically chosen as the template and despite the low sequence identity of 36%, the model showed a good Z-score of −0.321. Notably, we found a high degree of structural conservation in the substrate access tunnel and especially the active site: 30 of 44 residues (68%) found in a vicinity of 10 Å around P450 BM3's Phe87, which is located centrally in the tunnel, are identical. In order to investigate whether this structural similarity would translate into
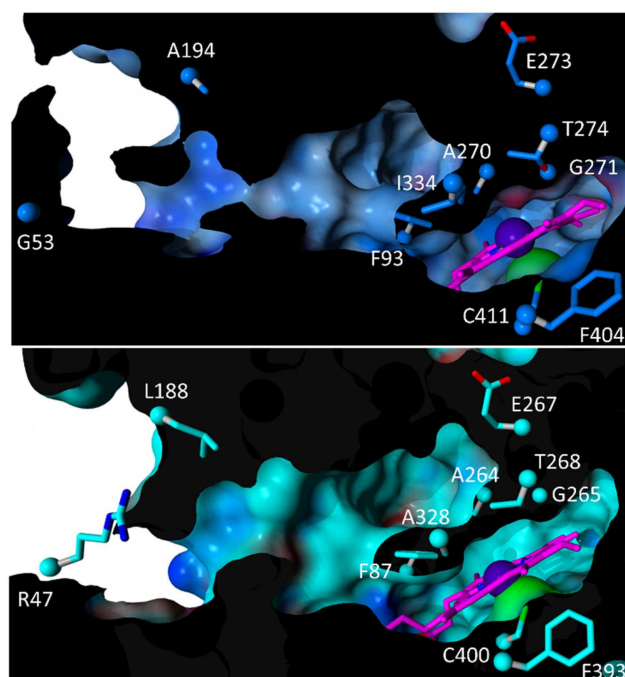
Figure 2. Access tunnel and active site of a homology model of CYP505A30 (top panel), compared with P450-BM3 crystal structure (PDB code 1FAG, bottom panel). The protein is shown with blue (CYP505A30) or cyan (BM3) carbons as sticks and the corresponding surfaces are cut open at various planes (black). The heme cofactor is pink and the central iron atom is violet.

selectivity similarity, we created variants of CYP505A30 based on P450-BM3 mutants described in literature. We chose one of the first P450-BM3 mutants reported to show activity on drug-like molecule – a triple mutant targeting both the active site as well as its access tunnel,[26] and a variant with two additional mutations found by directed evolution, named M01 in P450-BM3, which showed a further increased activity towards several substrates.[27]

The mutations of the two variants, their position in P450-BM3, and the homologous positions targeted in CYP505A30 can be found in Table 1. One of the residues is a phenylalanine located directly above the heme (F87 in P450-BM3), which is assumed to be
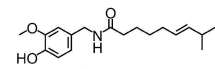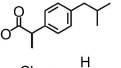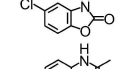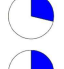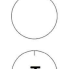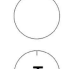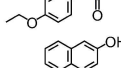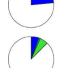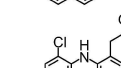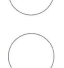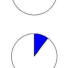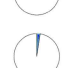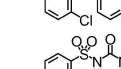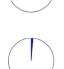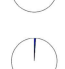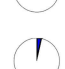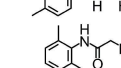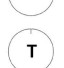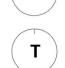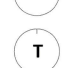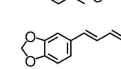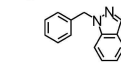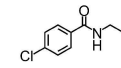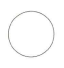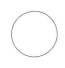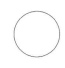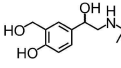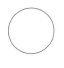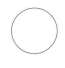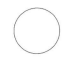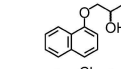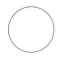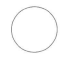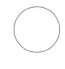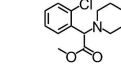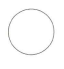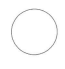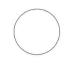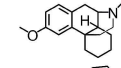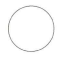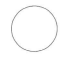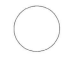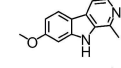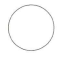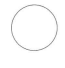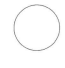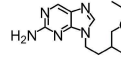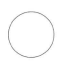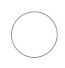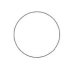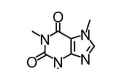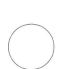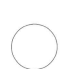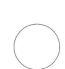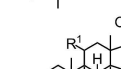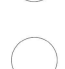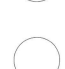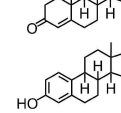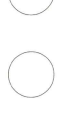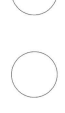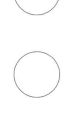
Table 1. Mutations of CYP505A30 variants used in this study.

P450-BM3 residue	CYP505A30 residue	mutated to	triple mutant (M3x)	quintuple mutant (M5x)
Arg47	Gly53	Leu	x	x
Phe87	Phe93	Val	x	x
Leu188	Ala194	Asp	x	x
Glu267	Glu273	Val		x
Gly415	Ala426	Ser		x

critical for the acceptance of larger substrates. This residue is conserved in both proteins, as is an active site glutamate (BM3: E267, CYP505A30: E273) whose exact role is still under debate.[5b] Two residues are located at the tunnel entrance: P450-BM3's Leu188, whose hydrophobic nature is retained in CYP505A30's Ala194, and Arg47, corresponding to the very different Gly53 in CYP505A30. The fifth position, Gly415 (corresponding to Ala426 in CYP505A30) has probably no influence on the activity alterations found in P450-BM3-M01[27] and was only added for a more realistic comparison. Wild-type CYP505A30 and the triple and quintuple mutants were then screened for activity on a panel of 21 active pharmaceutical ingredients (APIs) using a previously described whole cell conversion assay.[28] Control reactions were performed with cells harboring the same vector lacking the P450 gene. The compounds and the conversion results are listed in Table 2.

Interestingly, we found that the mutations only slightly affected the substrate scope of CYP505A30, while they had a distinct effect on the product distribution. All three variants oxidized eight compounds, of which the two best substrates were capsaicin and ibuprofen. Capsaicin is the pungency-causing compound in chili peppers, and is undergoing clinical trials as a therapeutic agent for various diseases.[29] Ibuprofen is a synthetic, nonsteroidal anti-inflammatory drug that finds widespread application as an over-the-counter analgesic.[30] Structurally, the two molecules show some similarity, as they are both composed of an aromatic ring and an aliphatic chain with a terminal isobutyl moiety (Table 2). Other compounds that were converted by all variants were the structurally diverse phenacetin, 2-naphthol, and tolbutamide. Phenacetine as well as chlorzoxazone were only converted in considerable amounts by the wild type, while diclofenac was only accepted by the mutants. For those cases, the reaction occurred selectively and yielded only one product. Lidocaine and piperine were converted in trace amounts by all three variants. Capsaicin was most efficiently converted by the wild-type enzyme, with 94.7% of the starting material being turned over. By comparison of the HPLC chromatograms with authentic standards prepared and reported recently,[28b] the major product could be identified as 8-hydroxycapsaicin, amounting to 81% of the total products. The second most abundant product (11%) resulted from epoxidation of the double bond. Although producing similar relative amounts of 8-hydroxycapsaicin, the M3x and M5x mutants produced higher amounts of an unidentified compound with identical mass to 8-hydroxycapsaicin, likely the product of hydroxylation at another position. The overall conversion yield was reduced to 73.6% and 32.6%, respectively. A reduction of the conversion yield from 43.1% to 10.4% was also observed for the

Table 2. Conversion of APIs by CYP505A30.

Substrate	Structural formula	MW[a]	Conversion[b] WT	M3x	M5x
Capsaicin		305			
Ibuprofen		206			
Chlorzoxazone		170			
Phenacetin		179		T	T
2-Naphthol		144			
Diclofenac		296			
Tolbutamide		270			
Lidocaine		234	T	T	T
Piperine		285	T	T	T
Benzydamine		309			
Moclobemide		269			
Salbutamol		239			
(±)-Propranolol		244			
Clopidogrel		322			
Dextromethorphan		271			
Harmine		212			
Famciclovir		321			
Caffeine		194			
Progesterone, Hydrocortisone[c]		314, 362			
Estriol		288			

[a] MW = Molecular weight.
[b] Products are depicted as percentages in various colors, unconverted substrate is depicted white. T = trace amounts converted.
[c] Progesterone: R[1], R[3] = H, R[2] = CH₃; Hydrocortisone: R[1] = OH, R[2] = CH₂OH, R[3] = OH

oxidation of ibuprofen by the M3x mutant, whereas the M5x mutant still converted 37.5%. Furthermore, in contrast to the wild type, which produced approximately equal amounts of three different products, M5x predominantly catalyzed the formation of one product (77.3%).

To determine the structure of the three ibuprofen metabolites, whole cell biooxidation was studied in a 200 mL preparative scale experiment using ibuprofen
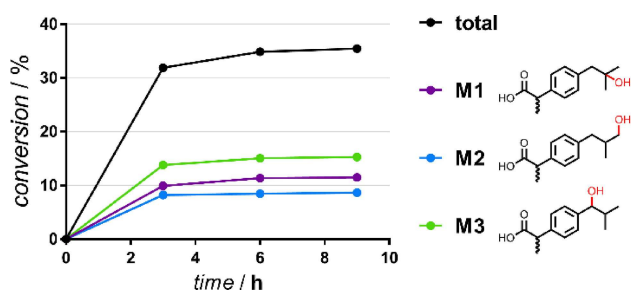
Figure 3. Preparative scale whole cell biooxidation of ibuprofen by CYP505A30. Reaction volume: 200 mL; substrate concentration: 3.75 mM. Conversion of ibuprofen gave three products (M1-M3) according to HPLC/MS. The sum of M1 to M3 represents the overall total conversion yield. The three monooxygenation products (221 g mol⁻¹; ESI, neg, SIM) are 2-hydroxy-ibuprofen (M1), 3-hydroxy-ibuprofen (M2) and 1-hydroxy-ibuprofen (M3) according to NMR (Figures S4–9).

in a concentration of 3.75 mM (~150 mg). Several samples were analyzed by HPLC/MS over a period of 9 hours and a final total conversion level of 35% was achieved. Notably, 32% total conversion was already reached after 3 hours. In agreement with analytical scale experiments, ibuprofen was oxidized to 3 metabolites, to an extent of 11% (metabolite 1), 9% (metabolite 2) and 15% (metabolite 3), respectively (Figure 3). According to HPLC/MS, all three metabolites had a mass of 221 g mol⁻¹ (ESI, neg, SIM), indicating mono-oxidation.[31] Cell emulsions were extracted with ethyl acetate and the metabolites were isolated by preparative reversed phase chromatography. Isolated products (M1–M3) were analyzed via 1D and 2D NMR spectroscopy and were confirmed to be 2-hydroxy-ibuprofen (M1), 3-hydroxy-ibuprofen (M2) and 1-hydroxy-ibuprofen (M3) (Figures 3, S4–9). These results are similar to biooxidations of ibuprofen with CYP505X from *Aspergillus fumigatus,* another homologue of P450-BM3.[28a] In line with its activity on lauric acid,[19] CYP505A30 preferentially oxidizes aliphatic side chains on (sub-)terminal positions; the API screen demonstrates, however, that oxidation is not restricted to such a structural element.

Conclusion

CYP505A30 could serve as a useful biocatalyst as it combines attractive features for application: it is a self-sufficient monooxygenase-reductase fusion enzyme that is moderately thermostable, shows low susceptibility to solvent exposure, and it can easily be heterologously expressed in soluble form. The enzyme shows a certain similarity to the well-established P450-BM3, although the stability of the two enzyme subdomains is inverted. CYP505A30's more stable reductase domain could therefore be used to generate a P450-BM3 chimera with improved thermostability, as

has been demonstrated previously.[32] It's broad pH-tolerance could furthermore prove useful in mechanistic or crystallographic studies. Its apparent high tolerance to cosolvents is a particularly useful feature for biooxidation of drugs, which are often large, hydrophobic molecules with poor water solubility. The basal activity on a surprisingly diverse range of compounds already found for the wild-type advocates CYP505A30's use as a starting point for directed evolution. Alternative enzymes are useful for early screens, as enzyme engineering is much more successful in expanding an initial (small) activity than introducing one from scratch.[33] (Semi)random mutagenesis and high-throughput activity screens to boost activity proved highly successful for P450-BM3,[4,5b] but our results suggest that a direct transfer of activities may not be achieved by simply copying mutations. As wild-type CYP505A30 already accepted several large drug-like molecules, it is maybe less surprising that our mutations had a smaller effect as anticipated. The results nevertheless demonstrate that besides substrate scope, active site mutagenesis can especially steer the product specificity.

Experimental Section

Materials

All standard reagents were purchased from Sigma Aldrich unless otherwise stated.

Plasmid Generation

A synthetic and codon optimized gene of a NCBI genbank entry XM_003663599 was ordered from GenScript (New Jersey, USA). The gene was ordered to be cloned via HindIII and XhoI in a pET28a vector with kanamycin resistance such that an N-terminal 6x-Histidine tag was translationally fused to CYP505A30. Plasmid integrity was confirmed by sequencing (GATC-Biotech, Germany).

Mutagenesis

The triple and quintuple mutants were generated using the multichange isothermal mutagenesis method.[34] Briefly, fully complementary forward and reverse primers were designed at the position that contained the mutation. PCR fragments from one position to the next were then created by combining forward and reverse primers of adjacent positions. The fragments were then assembled by Gibson cloning,[35] using an in-house prepared reaction mix. The assembled plasmid was transformed, and a re-isolated plasmid from a single colony was sent for sequencing to confirm the presence of the mutations.

Enzyme Expression and Purification

E. coli BL21 (DE3) competent cells were transformed with the pET28a-6xHis-CYP505A30 vector (or the mutated version) and the cells were plated on a Luria-Bertani (LB) agar plate

containing 50 µg/mL kanamycin. A single colony was picked and grown over night in $LB_{Kan.}$. The overnight culture was used to inoculate a main culture of terrific broth (TB) medium which was shaken in an Erlenmayer flask without baffles at 37 °C until an OD_{600} of approximately 1.8 was reached. Protein expression was then induced by addition of 1 mM IPTG, upon which the culture was shifted to 24 °C, where it was allowed to grow for another 18 h. Cells were harvested by centrifugation and either frozen at −20 °C or processed directly.

After resuspension in 50 mM Tris/HCl pH 7.4, cells were sonicated for 15 minutes and cell debris was removed by centrifugation. The cell free extract was loaded on a pre-equilibrated gravity flow column containing appropriate amounts of Ni^{2+} Sepharose HP (GEHealthcare). The column was incubated at 4 °C rotating for 1 h and the flow through discarded. The column was washed with 50 mM Tris/HCl pH 7.4 and 50 mM Tris/HCl pH 7.4 containing 5 mM imidazole. The protein was then eluted by washing the column with 50 mM Tris/HCl pH 7.4 containing 500 mM imidazole. Salt was removed by applying the solution to a pre-equilibrated Econo-Pac 10DG desalting column (Bio-Rad). For storage, 10% glycerol was added, the protein shock-frozen in liquid nitrogen and stored at −80 °C.

Spectra

CO-difference spectra were obtained by following the protocol of Guengerich et al.[36] and recorded on a V-660 Jasco spectrophotometer.

NADPH Consumption Assay

The reaction mix of 200 µL was buffered in 50 mM Tris/HCl pH 7.4 and contained 1 µM purified P450, 1 mM of lauric acid (except for the uncoupling measurement) and 100 µM NADPH (or NADH in an initial experiment). The assays were performed at room temperature. After addition of the cofactor, the mix was transferred to a cuvette and the reaction followed at 340 nm on a spectrophotometer (V-660 Jasco).

Bioconversion with Purified Enzyme and GC-MS Analysis

The bioconversion mix of 1 mL with purified enzyme was prepared in 50 mM Tris/HCl pH 7.4 and contained 1 µM purified P450, 1 mM of lauric acid and 100 µM NADPH. For cofactor regeneration, 1 µM purified thermostable phosphite dehydrogenase[23] and 10 mM phosphite were added. The mix was incubated at 30 °C in a closed 20 mL glass vial and mildly agitated for 24 h. The reaction was stopped by adding NaCl saturated 1 M HCl and subsequently equal amounts of ethyl acetate were added. After thorough mixing and centrifugation, the organic layer was removed and dried over anhydrous magnesium sulfate. 1% TMS in BSTFA was added and the sample incubated at 75 °C for 30 min. 1 µl was then injected in a GC-MS QP2010 ultra instrument (Shimadzu) with electron ionization and quadrupole separation, using an HP-1 column (Agilent, 30 m × 0.32 mm × 0.25 µm). The settings of the GC oven were 30 °C, wait 5 min, 5 °C/min ramp to 70, wait 5 min, 5 °C/min ramp to 130 °C, wait 5 min, 15 °C/min ramp to 325 °C, wait 7 min.

T_m Determination using a Fluorescent Shift Assay

To determine the apparent melting temperature (T_m) in different conditions, duplicate samples of 25 µl were prepared in a 96-well thin-walled PCR plate. The samples contained 1 mg/mL purified enzyme. The plate was heated from 20 °C to 90 °C, increasing temperature by 0.5 °C every 10 seconds, using an RT-PCR machine (CFX96-Touch, Bio-Rad Laboratories) that measured fluorescence using a 450–490 excitation filter and a 515–530 nm emission filter. The melting point was defined as the inflection point of the resulting melting curve, equivalent to the maximum of the first derivative of the same curve.

Three different buffers at 50 mM concentration were used to cover a wide pH range: sodium acetate for pH 3.6–5.6, sodium phosphate for pH 5.8.–8.0, and Tris/HCl for pH 7.4–9.0. Samples containing cosolvents were in 50 mM Tris/HCl pH 7.4.

Activity Assay in Varying Conditions

The same plate as for the T_m determination was prepared and diluted in a 96-well microtiter plate with the same buffer layout to achieve an enzyme concentration of 1 µM in each well. Activity was measured in a plate reader (Synergy MX microtiter plate reader, BioTek Instruments) with automatic dispensing of NAPDH (final concentration 100 µM) and lauric acid as a substrate (final concentration 1 mM) before measuring absorbance at 340 nm for 1 min.

Whole Cell Conversions of APIs

Frozen cells were thawed and resuspended in potassium phosphate buffer (100 mM pH 7.4, 8.5% w/v sucrose) in 24-well plates. Trisodium citrate (50 µL, 1 M in ddH2O), $NADP^+$ (50 µL, 1 mM in ddH2O), $MgCl_2$ (10 µL, 1 M in ddH2O), glucose (10 µL, 1 M in ddH2O), and GDH (5 µL, 10 mg mL-1 in ddH2O) were added to 825 µL of cell suspension. The reaction was started by the addition of substrate (50 µL, 100 mM in DMSO). The final cell density at 600 nm (OD_{600}) was 100 in a total volume of 1 mL. The plate was sealed with gas permeable adhesive seal and incubated at 30 °C and 120 rpm in an orbital shaker for 16 h. The reactions were terminated by the addition of MeOH/ACN (1 mL 1:1 v/v). After mixing, the reaction mix was centrifuged in a 1.5 mL Eppendorf tube (5 min, 4 °C, 13,400 rpm). 200 µL of the supernatant were analyzed in polypropylene microtiter plates by HPLC-MS on a 1200 HPLC Series equipped with G1379B degasser, G1312B binary pump, SL G1367C HiP-ALS SL autosampler, G1314C VWD SL UV detector, G1316B TCC SL column oven and G1956B mass selective detector (MSD) with a Kinetex 50× 4.6 mm; 2.6u; C18; 100 An HPLC column (Phenomenex) equipped with a UHPLC C18 Security Guard ULTRA cartridge (Phenomenex).

Scale up Reactions

CYP505A30 wild type was studied on preparative scale. Preparative scale bioconversions were performed in baffled 2 L Erlenmayer flasks in a total reaction volume of 200 mL (optical density at 600 nm (OD_{600}) corresponding to 100). 154 mg ibuprofen (dissolved in 25 mL of DMSO) were used as the substrate (3.75 mM). Ibuprofen biooxidation was monitored for 9 hours. Unreacted ibuprofen and its metabolites were extracted with EtOAc. The solvent of the combined organic layers was removed under reduced pressure. Ibuprofen was separated from the metabolites by silica gel chromatography. Metabolite compounds were separated via reverse phase HPLC on a Thermo Scientific Dionex Ulti Mate 3000 Instrument using a Macherey-Nagel VP 125/21 Nucleodur 100–5 C18 EC column. A linear gradient of 2% to 65% MeCN in 24 min was used. 1D and 2D NMR spectroscopy (^{1}H, ^{13}C, APT, COSY, HSQC, HMBC) were recorded on a Bruker AVANCE III 300 spectrometer with autosampler (^{1}H: 300.36 MHz; ^{13}C: 75.53 MHz) and chemical shifts are referenced to residual protonated solvent signals as internal standard. To facilitate the interpretation, the C-spectra were proton decoupled to gain better identification of the peaks.

Homology Model

The homology model of CYP505A30 was created using YASARA version 15.11.18. The amino acid sequence in a FASTA format was used as an input, and the program's hm_build.mcr macro was used with standard settings.[37] The model was mainly built on the P450-BM3 structure with pdb code 1ZO9,[38] while some parts were the result of hybridization with models built based on pdb codes 2IJ3, 3KX3, and 1ZO4. The overall quality Z-score of the model was −0.321, which is judged "good" by YASARA.

Acknowledgements

References

[1] J. A. Labinger, J. E. Bercaw, *Nature* **2002**, *417*, 507–514.

[2] I. G. Denisov, T. M. Makris, S. G. Sligar, I. Schlichting, *Chem. Rev.* **2005**, *105*, 2253–2278.

[3] F. P. Guengerich, in *Cytochrome P450*, Springer, Berlin, **2005**, pp. 377–530.

[4] G. Grogan, *Curr. Opin. Chem. Biol.* **2011**, *15*, 241–248.

[5] a) A. W. Munro, H. M. Girvan, K. J. McLean, *Nat. Prod. Rep.* **2007**, *24*, 585–609; b) C. J. Whitehouse, S. G. Bell, L.-L. Wong, *Chem. Soc. Rev.* **2012**, *41*, 1218–1260.

[6] F. Hannemann, A. Bichet, K. M. Ewen, R. Bernhardt, *Biochim. Biophys. Acta Gen. Subj.* **2007**, *1770*, 330–344.

[7] G. D. Nordblom, R. E. White, M. J. Coon, *Arch. Biochem. Biophys.* **1976**, *175*, 524–533.

[8] M. J. Coon, *Annu. Rev. Pharmacol. Toxicol.* **2005**, *45*, 1–25.

[9] L. O. Narhi, A. J. Fulco, *J. Biol. Chem.* **1986**, *261*, 7160–7169.

[10] R. Bernhardt, *J. Biotechnol.* **2006**, *124*, 128–145.

[11] K. G. Ravichandran, S. S. Boddupalli, C. Hasermann, J. A. Peterson, J. Deisenhofer, *Science* **1993**, *261*, 731–736.

[12] K. Zhang, B. M. Shafer, M. D. Demars, H. A. Stern, R. Fasan, *J. Am. Chem. Soc.* **2012**, *134*, 18695–18704.

[13] G. Di Nardo, G. Gilardi, *Int. J. Mol. Sci.* **2012**, *13*, 15901.

[14] W. N. Kühn-Velten, *Z. Naturforsch. C* **1997**, *52*, 132–136.

[15] N. Doukyu, H. Ogino, *Biochem. Eng. J.* **2010**, *48*, 270–282.

[16] A. W. Munro, J. Gordon Lindsay, J. R. Coggins, S. M. Kelly, N. C. Price, *Biochim. Biophys. Acta* **1996**, *1296*, 127–137.

[17] a) O. Salazar, P. C. Cirino, F. H. Arnold, *ChemBioChem* **2003**, *4*, 891–893; b) T. Seng Wong, F. H. Arnold, U. Schwaneberg, *Biotechnol. Bioeng.* **2004**, *85*, 351–358.

[18] M. T. Lundemo, J. M. Woodley, *Appl. Microbiol. Biotechnol.* **2015**, *99*, 2465–2483.

[19] G. J. Baker, H. M. Girvan, S. Matthews, K. J. McLean, M. Golovanova, T. N. Waltham, S. E. J. Rigby, D. R. Nelson, R. T. Blankley, A. W. Munro, *ACS Omega* **2017**, *2*, 4705–4724.

[20] M. J. L. J. Fürst, S. Savino, H. M. Dudek, J. R. Gomez Castellanos, C. Gutierrez de Souza, S. Rovida, M. W. Fraaije, A. Mattevi, *J. Am. Chem. Soc.* **2017**, *139*, 627–630.

[21] Y. Marin-Felix, A. M. Stchigel, A. N. Miller, J. Guarro, J. F. Cano-Lira, *Mycologia* **2015**, *107*, 619–632.

[22] a) S. Fuziwara, I. Sagami, E. Rozhkova, D. Craig, M. A. Noble, A. W. Munro, S. K. Chapman, T. Shimizu, *J. Inorg. Biochem.* **2002**, *91*, 515–526; b) B. Rowlatt, J. A. Yorke, A. J. Strong, C. J. Whitehouse, S. G. Bell, L.-L. Wong, *Protein Cell* **2011**, *2*, 656–671.

[23] T. W. Johannes, R. D. Woodyer, H. Zhao, *Biotechnol. Bioeng.* **2007**, *96*, 18–26.

[24] F. Forneris, R. Orru, D. Bonivento, L. R. Chiarelli, A. Mattevi, *FEBS J.* **2009**, *276*, 2833–2840.

[25] R. T. Ruettinger, A. J. Fulco, *J. Biol. Chem.* **1981**, *256*, 5728–5734.

[26] B. M. Lussenburg, L. C. Babel, N. P. Vermeulen, J. N. Commandeur, *Anal. Biochem.* **2005**, *341*, 148–155.

[27] B. M. van Vugt-Lussenburg, E. Stjernschantz, J. Lastdrager, C. Oostenbrink, P. Vermeulen, J. N. Commandeur, *J. Med. Chem.* **2007**, *50*, 455–461.

[28] a) C. Rinnofner, B. Kerschbaumer, H. Weber, A. Glieder, M. Winkler, *Biocatal. Agric. Biotechnol.* **2019**, *17*, 525–528; b) A. K. Migglautsch, M. Willim, B. Schweda, A. Glieder, R. Breinbauer, M. Winkler, *Tetrahedron* **2018**, *74*, 6199–6204.

[29] P. Patowary, M. P. Pathak, K. Zaman, P. S. Raju, P. Chattopadhyay, *Biomed. Pharmacother.* **2017**, *96*, 1501–1512.

[30] J. J. Prusakiewicz, K. C. Duggan, C. A. Rouzer, L. J. Marnett, *Biochemistry* **2009**, *48*, 7353–7355.

[31] I. Neunzig, A. Göhring, C.-A. Drăgan, J. Zapp, F. T. Peters, H. H. Maurer, M. Bureik, *J. Biotechnol.* **2012**, *157*, 417–420.

[32] S. Eiben, H. Bartelmäs, V. B. Urlacher, *Appl. Microbiol. Biotechnol.* **2007**, *75*, 1055–1061.

[33] S. G. Peisajovich, D. S. Tawfik, *Nat. Methods* **2007**, *4*, 991.

[34] L. A. Mitchell, Y. Cai, M. Taylor, A. M. Noronha, J. Chuang, L. Dai, J. D. Boeke, *ACS Synth. Biol.* **2013**, *2*, 473–477.

[35] D. G. Gibson, in *Methods Enzymol., Vol. 498* (Ed.: C. Voigt), Academic Press, New York, NY, **2011**, pp. 349–361.

[36] F. P. Guengerich, M. V. Martin, C. D. Sohl, Q. Cheng, *Nat. Protoc.* **2009**, *4*, 1245–1251.

[37] E. Krieger, K. Joo, J. Lee, J. Lee, S. Raman, J. Thompson, M. Tyka, D. Baker, K. Karplus, *Proteins* **2009**, *77 (Suppl 9)*, 114–122.

[38] A. Hegde, D. C. Haines, M. Bondlela, B. Chen, N. Schaffer, D. R. Tomchick, M. Machius, H. Nguyen, P. K. Chowdhary, L. Stewart, *Biochemistry* **2007**, *46*, 14010–14017.

M. J. L. J. Fürst, B. Kerschbaumer, C. Rinnofner, A. K. Migglautsch, M. Winkler, M. W. Fraaije*